

# Impact of a Wedge-Shaped Body with Influence of Broken Ice

Kevin J. Maki<sup>1</sup>, Haixuan Ye<sup>1</sup>, T.I. Khabakhpasheva<sup>2</sup>, A.A. Korobkin<sup>2</sup>

<sup>1</sup> Department of Naval Architecture and Marine Engineering, University of Michigan, Ann Arbor, MI, 48109 USA,  
e-mail: kjmaki@umich.edu, hxye@umich.edu

<sup>2</sup> School of Mathematics, University of East Anglia, Norwich, UK, e-mail: t.khabakhpasheva@uea.ac.uk,  
a.korobkin@uea.ac.uk

## Introduction

As the climate on Earth evolves the access to open water in the Arctic is steadily increasing. This imposes new opportunities for operation of commercial and naval ships in this unique environment. It is desirable to design, build, and operate ships that can operate reliably in a wide range of icy conditions found in the Arctic. In order to understand the contribution of ice on the operation and reliability of a ship, it is important to quantify the influence of ice on the loads experienced by the ship. This abstract is focused predicting the slamming loads on a ship that is operating in water with broken ice.

Most of our current knowledge about slamming loads on ships in open water is based upon the early ideas of von Karman[1] and Wagner[4] who studied the simple problem of a wedge entering the water vertically with constant velocity. The selection to study simple problem laid the foundation for the substantial body of work that followed. While the water is rather easy to characterize, indeed only a single parameter of the mass density is needed, the characterization of ice is far more complicated. Ice is many different topologies such as sheets, packs, brash, or broken ice. It can be thought of as a structure with non-homogeneous and nonlinear properties that vary significantly depending on the age and climate conditions. It is brittle and the fracture and breakup process is very complicated. To analyze the distribution of types of ice some researchers have treated the impact of ice from a statistical viewpoint[5]. In this work we consider a single piece of ice and analyze the force and pressure distribution on a wedge entering the water with constant velocity. The ice may vary in size and location relative to the wedge. Also, the ice may be considered to be floating and free to move, or, fixed in space.

## Theoretical model of water entry through broken ice

The two-dimensional Wagner model of water entry is generalised to account for several ice floes floating near the place of impact. Both the ice floes and the impact region are approximated with flat plates of zero drafts,  $(a_j, b_j)$ , on the boundary,  $y = 0$ , of deep water,  $y < 0$ . The number of the plates is  $N + 1$ , where  $N$  is the number of floes. The plates are separated with intervals of free surface. One of the plate, say  $j = k$ , corresponds to the contact region between the solid body,  $y = f(x) - h(t)$ , and the water, where  $f(x)$  describes the body shape,  $f(a_k(0)) = 0$ ,  $f(x) > 0$ , where  $x \neq a_k(0)$ , and  $h(t)$  is the penetration depth of the body,  $h(0) = 0$ . The contact region,  $a_k(t) < x < b_k(t)$ , expands in time,  $a_k(0) = b_k(0)$  at the impact time  $t = 0$ . The end points of the contact region,  $a_k(t)$  and  $b_k(t)$ , should be determined as part of the solution from the condition that the liquid displacement at these two points is finite. The ice floes can move only vertically and rotate with their end point  $a_j$  and  $b_j$ ,  $j \neq k$  being stationary in time. The small displacement of the  $j$ -th flow is described by the equation  $y = h_j(t) + \alpha_j(t)(x - x_{jc})$ , where  $x_{jc} = (a_j + b_j)/2$  is the centre of the floe,  $h_j(t)$  is the vertical displacement of this centre, and  $\alpha_j(t)$  is the angular rotation of the  $j$ -th floe. The functions  $h_j(t)$  and  $\alpha_j(t)$  are unknown in advance and should be determined as part of the solution.

The linearised problem of water entry is solved by using the displacement potential  $\phi(x, y, t)$  and the complex displacement  $W(z) = \phi_x - i\phi_y$ , where  $z = x + iy$ ,  $\phi_x$  and  $\phi_y$  are the horizontal and vertical components of the liquid displacement correspondingly. The complex displacement  $W(z)$  is an analytic function in the flow region,  $y < 0$ , and satisfies the boundary conditions  $\phi_y = h_j(t) + \alpha_j(t)(x - x_{jc})$  on the intervals  $a_j < x < b_j$ ,  $j \neq k$ , and  $\phi_y = f(x) - h(t)$ , where  $a_k(t) < x < b_k(t)$ . On the intervals of the free surface between the plates,  $\phi_x = 0$ , which follows from the dynamic boundary condition. In addition,  $\phi = 0$  on the free surfaces. The analytic function  $W(z)$  is obtained by using the characteristic functions of the solid parts of the liquid boundary,  $R_j(z) = \sqrt{(z - a_j)(z - b_j)}$ . On the boundary,  $z = x - i0$ , we have  $R_j(x - i0) = r_j(x)$ , where  $r_j(x) = \sqrt{(x - a_j)(x - b_j)}$  for  $x > b_j$  and  $r_j(x) = -\sqrt{(a_j - x)(b_j - x)}$  for  $x < a_j$ . In the  $j$ -th interval,  $R_j(x - i0) = -ir_j(x)$ , where  $r_j(x) = \sqrt{(x - a_j)(b_j - x)}$  for  $a_j < x < b_j$ . The product  $R(z) = \prod_{j=1}^{N+1} R_j(z)$  is analytic in the flow region, its imaginary part is zero on the free-surface intervals of the boundary, and on the solid part of the boundary,  $R(x - i0) = -i \prod_{j=1}^{N+1} r_j(x) = -ir(x)$ , where  $r_j(x)$  are real functions. It is known that  $R(z) = O(z^{N+1})$  and  $W(z) = O(z^{-2})$  as  $z \rightarrow \infty$ . The product  $W(z)R(z)$  is analytic in  $y < 0$  and can

be written as  $WR(z) = -i(C_0 + C_1z + \dots + C_{N-1}z^{N-1}) + U(z)$ , where  $U(z) \rightarrow 0$  as  $z \rightarrow \infty$  and  $C_n$  are real coefficients to be determined. The Hibert formula

$$\text{Im}[U(x - i0)] = \frac{1}{\pi} P_v \int_{-\infty}^{\infty} \frac{\text{Re}[U(\tau - i0)] d\tau}{\tau - x}$$

gives the horizontal displacements,  $\phi_x(x, 0, t)$ , along the  $j$ -th solid part of the boundary

$$\phi_x(x, 0, t)r(x) = \frac{1}{\pi} \sum_{n=1}^{N+1} \int_{a_n}^{b_n} \frac{\phi_y(\tau, 0, t)r(\tau)d\tau}{\tau - x} + C_0 + C_1x + \dots + C_{N-1}x^{N-1} \quad (a_j < x < b_j). \quad (1)$$

The coefficients  $C_n$  are determined from the condition that  $\phi(x, 0, t) = 0$  between any two solid plates. This condition provides  $N$  equations for  $N$  coefficients  $C_n$ ,

$$\int_{a_j}^{b_j} \phi_x(x, 0, t) dx = 0 \quad (1 \leq j \leq N + 1, j \neq k), \quad (2)$$

where  $\phi_x(x, 0, t)$  is given by (1). The motions  $h_j(t)$  and  $\alpha_j(t)$  of the the  $j$ -th floe are governed by the Newton second law, where the force is given by

$$F_j(t) = \rho \frac{d^2}{dt^2} \left( \int_{a_j}^{b_j} x \phi_x(x, 0, t) dx \right).$$

The motion equations can be twice integrated in time with the result

$$\rho_i(b_j - a_j)h_j = \int_{a_j}^{b_j} x \phi_x(x, 0, t) dx, \quad (3)$$

where  $\phi_x(x, 0, t)$  is given by (1). Equations (2), (3) and similar equations for the angular motions of the floes form the linear system of  $3N$  algebraic equations with respect to  $3N$  unknown functions of time  $C_{j-1}(t)$ ,  $h_j(t)$  and  $\alpha_j(t)$ , where  $1 \leq j \leq N + 1, j \neq k$ . The coefficients and the right-hand sides of this system depend on time  $t$  through the positions of the contact points  $a_k(t)$  and  $b_k(t)$  and the penetration depth  $h(t)$ , and they are given by double integrals, which makes their evaluation challenging. Finally the motion of the contact points,  $a_k(t)$  and  $b_k(t)$ , are determined by using the Wagner condition that the displacements are finite at these points. This condition and the equation (1) yield that the right-hand side in (1) is equal to zero at  $x = a_k(t)$  and at  $x = b_k(t)$ . Note that the displacements of liquid are not finite at the ends of the ice floes. The resulting system of  $3N + 2$  equations is linear with respect to  $C_{j-1}(t)$ ,  $h_j(t)$  and  $\alpha_j(t)$  and nonlinear with respect to the positions of the contact points,  $a_k(t)$  and  $b_k(t)$ . It is interesting to notice that the time is a parameter in this system. Therefore, the positions of the ice floes and the size of the contact region at each time instant do not depend on the history of the flow but only on the positions of the floes, shape of the body and its penetration depth. Results of the calculations in this model will be presented at the workshop.

## Computational Fluid Dynamics Method

High-fidelity computations are performed for a wedge entering the water with constant velocity in the proximity of a single piece of ice. The numerical solver is based on the OpenFOAM open-source CFD toolkit. The air and water are assumed to be governed by the incompressible Navier-Stokes equations. A volume-of-fluid method is used to track the air-water interface. For constant-velocity impact the solution may be obtained in either the body or earth-fixed coordinate systems, both of which are inertial. Validation for the impact in water only has been done extensively by the current authors and many others[2, 3]. Different modeling strategies are used for the fixed or floating ice. For fixed ice, an immersed-boundary method is implemented. For floating ice, a fictitious-fluid approach is employed.

The incompressible Navier-Stokes equations are

$$\partial_t \rho \mathbf{u} + \nabla \cdot \rho \mathbf{u} \mathbf{u} = -\nabla p + \rho \mathbf{g} + \nabla \cdot 2\mu \mathbf{S} + \mathbf{f} \quad \nabla \cdot \mathbf{u} = 0 \quad (4)$$

where  $\mathbf{u}$  is the fluid velocity,  $p$  is the pressure,  $\mathbf{S}$  is the strain-rate tensor. The additional source term  $\mathbf{f}$  is zero except in the case of the immersed-boundary method. The acceleration of gravity vector is  $\mathbf{g}$ . The fluid mechanical properties of mass density  $\rho$  and molecular viscosity  $\mu$  vary in space and time depending on the phase-fraction variable  $\alpha$  as  $\rho(\mathbf{x}, t) = \alpha_1(\mathbf{x}, t)\rho_{\text{water}} + \alpha_2(\mathbf{x}, t)\rho_{\text{air}}$  and  $\mu(\mathbf{x}, t) = \alpha_1(\mathbf{x}, t)\mu_{\text{water}} + \alpha_2(\mathbf{x}, t)\mu_{\text{air}}$ .

The phase fraction variable satisfies the conservation of mass equation as:

$$\frac{D\alpha_1}{Dt} = \frac{\partial \alpha_1}{\partial t} + \nabla \cdot \alpha_1 \mathbf{u} = 0 \quad \text{and} \quad \alpha_1 + \alpha_2 = 1 \quad (5)$$

**Modeling of stationary ice** In the case of the ice being fixed in space the immersed-boundary method is used. The term  $\mathbf{f}(\mathbf{x})$  found in the Navier-Stokes equations (4) is expressed as:  $\mathbf{f}(\mathbf{x}) = -C(\mathbf{x})(\mathbf{u} - \mathbf{v})$ . where  $C(\mathbf{x})$  is a coefficient that is zero outside of the ice region of the domain, and it takes a value of  $10^6$  inside the ice region. The vector  $\mathbf{v}$  is the desired velocity of the ice. This large source term is treated implicitly for numerical stability reasons, and has the effect of forcing the fluid velocity to the velocity of the ice, which is zero in this case.

**Modeling of floating ice** For floating ice the entire domain outside of the body is considered to be fluid. This includes the region of the ice, and thus the domain consists of three phases: water, air, and ice. In the region of space where there is ice, the fluid properties are taken to be the density of ice, but with an artificially high value of the molecular viscosity. This has the influence of maintaining very low strain-rate for a given applied fluid stress. Due to the short time duration of the impact event, the low strain-rate produces low strain, and the fluid that represents the ice moves mostly as a rigid body. This approach is only suitable for short-time duration events.

The solution of the three phases follows the same basic procedure that is used for the two-phase simulation. In the case of three-phases, an additional transport equation is added for the second volume fraction. The phase-indicator function for each constituent is found from the three equations:

$$\frac{\partial \alpha_1}{\partial t} + \nabla \cdot \alpha_1 \mathbf{u} = 0; \quad \frac{\partial \alpha_2}{\partial t} + \nabla \cdot \alpha_2 \mathbf{u} = 0; \quad \sum \alpha_i = \alpha_1 + \alpha_2 + \alpha_3 = 1, \quad (6)$$

and the spatially varying mechanical properties are found as:  $\rho(\mathbf{x}, t) = \alpha_1 \rho_{\text{water}} + \alpha_2 \rho_{\text{air}} + \alpha_3 \rho_{\text{ice}}$  and  $\mu(\mathbf{x}, t) = \alpha_1 \mu_{\text{water}} + \alpha_2 \mu_{\text{air}} + \alpha_3 \mu_{\text{ice}}$ . The parameters for each fluid are found in Table 1.

## Results

For floating ice the fictitious-fluid method is used. Three wedge deadrise angles are studied: 10, 20, 30 degrees. The wedge beam for all is  $B = 2$  m. The impact velocity 2 m/s. The domain dimensions are width of  $6B$ , and depth of  $5B$ . Gravity is  $9.81 \text{ m/s}^2$ , although it should be negligible for this impact velocity and wedge size. The dimensions of the ice are 0.8 by 0.1 m. The spacing between the ice and edge of wedge is 0.2 m or  $0.1B$ . Ice density of  $930 \text{ kg/m}^3$  is used, and the ice is initially level with calm-water surface.

Figure 1 shows the force time history for the floating ice cases. For reference the force is also shown for the case without ice. For this configuration the increase in force is shown to be about 20%, and the maximum increase occurs at the instant of chine wetting. Figure 2 shows the pressure field for each wedge. The ice is seen colored in red. The presence of the ice is seen to increase the pressure on the side of the wedge.

For stationary ice the 20 degree wedge is used and 4 different configurations of ice are studied. The thickness is 0.1 m, and the length of ice is 0.25, 0.5, 1.0, and 2.0 m. The edge closest to the wedge is constant and equal to 0.2 m, just as in the floating-ice case. The time history for the stationary ice is shown in Figure 3. Also for reference the forces for the no ice and the stationary ice (with length 0.8 m) cases are shown. The increase in force due to stationary ice is very similar to that of floating ice. As the length of the ice increases, so does the force. After the time of chine wetting the force for the stationary ice returns rapidly to that of the no-ice condition. This is because the floating ice travels upwards and away from the body and as such its influence on the body is decreased.

For the workshop we will show comparison to a theory that can predict the force on the body. Also, we will show additional cases that show the influence of the proximity of the ice to the body on the force.

**Acknowledgements** The authors would like to gratefully acknowledge the U.S. Office of Naval Research for the support of this work.

## References

- [1] T. von Karman. The impact on seaplane floats during landing. Technical Notes 321, NACA, 1929.
- [2] K. J. Maki, D. Lee, A. W. Troesch, and N. Vlahopoulos. Hydroelastic impact of a wedge-shaped body. *Ocean Engineering*, 38:621–629, 2011.
- [3] D. Piro and K. Maki. Hydroelastic analysis of bodies that enter and exit water. *Journal of Fluids and Structures*, 37:134–150, 2013.
- [4] V. H. Wagner. Über Stoß und Gleitvorgänge an der Oberfläche von Flüssigkeiten. *Zeitschrift Für Angewandte Mathematik Und Mechanik (ZAMM)*, 12, August 1932.
- [5] B. Su, K. Riska, and T. Moan. Numerical simulation of local ice loads in uniform and randomly varying ice conditions. *Cold Regions Science and Technology*, 65:145–159, 2011.

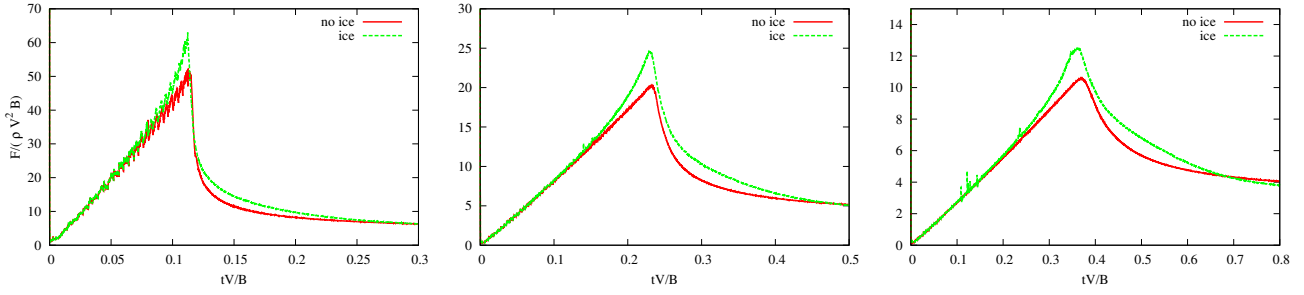


Figure 1: Comparison of force, (left) 10 deg, (center) 20 deg, (right) 30 deg

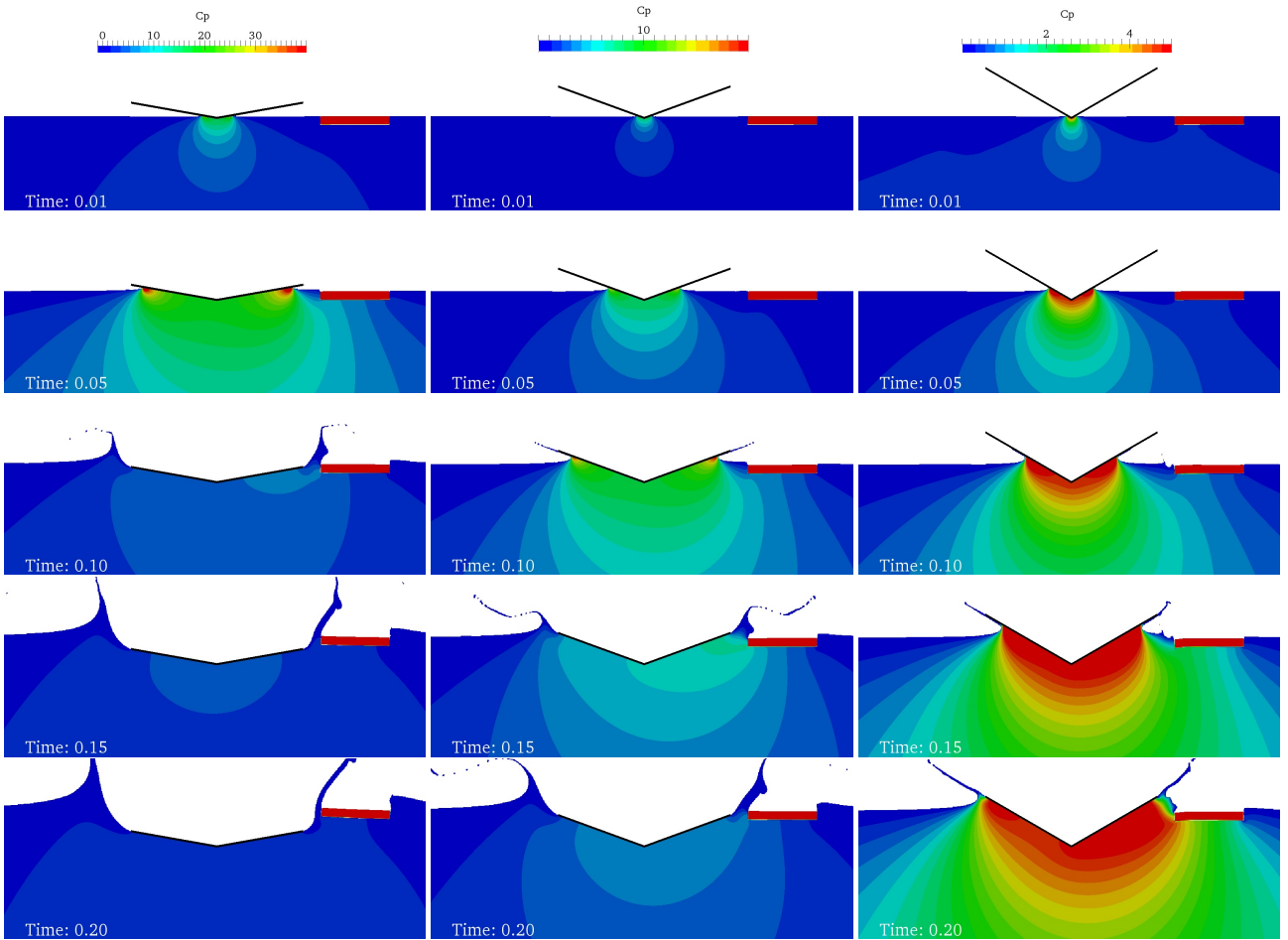


Figure 2: Pressure coefficient, (left) 10 deg, (center) 20 deg, (right) 30 deg

Fluid	Density (kg/m <sup>3</sup> )	Viscosity (m <sup>2</sup> /s)
water	1000	$1 \times 10^{-6}$
air	1.2	$1.5 \times 10^{-5}$
ice	930	100

Table 1: Fluid properties

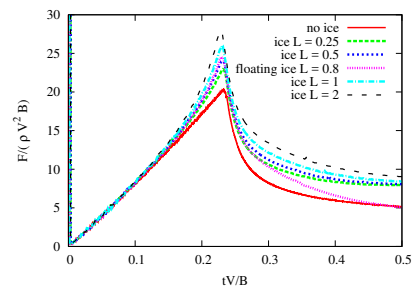


Figure 3: Force time history for stationary ice